Acta Crystallographica Section D
Biological Crystallography
ISSN 0907-4449

Purification, crystallization and preliminary X-ray analysis of the soluble domain of the Na^+-pumping cytochrome *bo* quinol oxidase from *Vitreoscilla*

Kyung-Jin Kim,[a,b] Youngchang Kim,[c] Kyung-Won Park,[b] Dale A. Webster[b] and Andrew J. Howard[a,b]*

[a]Industrial Macromolecular Crystallography Association Collaborative Access Team (IMCA-CAT), Advanced Photon Source, Argonne National Laboratory, 9700 South Cass Avenue, Argonne, IL 60439, USA, [b]Department of Biological, Chemical and Physical Sciences, Illinois Institute of Technology, Chicago, IL 60616, USA, and [c]Biosciences Division, Structural Biology Center, Argonne National Laboratory, 9700 South Cass Avenue, Argonne, IL 60439, USA

Correspondence e-mail: howard@iit.edu

Received 21 February 2002
Accepted 8 April 2002

The 24 kDa CyoA soluble domain of *Vitreoscilla* cytochrome *bo* quinol oxidase, which pumps out Na^+ during respiration, has been crystallized from a solution of 2 *M* ammonium sulfate and 5% 2-propanol. The crystal belongs to cubic space group $P4_332$, with unit-cell parameters $a = b = c = 122.2$ Å, $\alpha = \beta = \gamma = 90^\circ$ and one subunit in the asymmetric unit. A 99.8% complete data set to 3.3 Å has been collected at the 17-ID beamline of the Advanced Photon Source. The structure was determined by molecular replacement and refinement is in progress.

1. Introduction

Cytochrome *bo* is one of the most widespread terminal oxidases in bacteria. The primary function of these oxidases is to conserve the energy generated in terminal respiration during the transfer of electrons to oxygen by pumping cations (usually H^+) across the membrane to establish a proton electrochemical gradient that can be used for ATP synthesis and other energy-requiring cellular processes (Saraste *et al.*, 1988; Gennis, 1991; Kita *et al.*, 1984; Matsushita *et al.*, 1984; Georgiou & Webster, 1987). Some microorganisms substitute Na^+ for H^+ as a direct coupling cation for ATP synthesis. Studies of cation transport during the respiration indicated that *Vitreoscilla* is an Na^+ motive organism, generating an Na^+ electrochemical gradient (inside negative) during terminal respiration (Efiok & Webster, 1990*a*). The cytochrome *bo* ubiquinol oxidase of this organism was identified as a primary Na^+ pump. Proteoliposomes containing cytochrome *bo* purified from *Vitreoscilla* translocate Na^+ when energized with substrate (Efiok & Webster, 1990*b*). Further evidence of the sodium-pumping function of *Vitreoscilla* cytochrome *bo* was also obtained using a *cyo*$^-$ knockout mutant (Kim *et al.*, 2000). This cytochrome *bo* terminal oxidase is homologous to the extensively studied *Escherichia coli* cytochrome *bo* (Georgiou *et al.*, 1988), except that the latter functions as an H^+ transporter. CyoB (subunit I of cytochrome *bo*) binds all the redox metal centers, hemes and Cu_B and has a high-affinity quinone-binding site (Trumpower & Gennis, 1994). The other quinol-binding site (low-affinity quinol-binding site) is located in the CyoA soluble domain (the C-terminal hydrophilic domain of subunit II) which is anchored to the membrane by two N-terminal transmembrane helices (Calhoun *et al.*, 1994; Gohlke *et al.*, 1997; Tsatsos *et al.*, 1998; Sato-Watanabe *et al.*, 1998; Wilmanns *et al.*, 1995). Tryptophan 136 in this subunit of *E. coli* cytochrome *bo* has been implicated in the binding of ubiquinol by biochemical assays (Ma *et al.*, 1998). To date, no structural studies have appeared providing direct evidence of the binding of ubiquinol to CyoA. It is expected that the structure of the *Vitreoscilla* CyoA soluble domain will provide a better understanding of the terminal oxidase system in this organism. Among the questions to be addressed are the role of the low-affinity quinol-binding site, the interactions between the CyoA soluble domain and the CyoB domain, and the differences between proton- and sodium-pumping oxidases. In this study, we report the cloning, expression, purification and X-ray crystallographic analysis of *Vitreoscilla* CyoA (subunit II) soluble domain.

2. Materials and methods

2.1. Cloning, expression and purification of *Vitreoscilla* CyoA soluble domain

A DNA fragment encoding the CyoA soluble domain was obtained by PCR amplification using the *Vitreoscilla* chromosome as a template. The upstream primer (5′-GCGCG-**GGATCC**ATACCGTCCATTGGATTCTG-3′) contained a *Bam*HI restriction site (bold) at its 5′ end and the downstream primer (5′-GCG-CG**AAGCTT**TTAATTTCCTCCTGCAGCA-GATGCAGC-3′) encoded a TAA stop codon and *Hin*dIII restriction site (bold). The 650 bp PCR product was digested with *Bam*HI/*Hin*dIII and ligated into *Bam*HI/*Hin*dIII-restricted pQE81 vector (Qiagen) to produce pVCAS. Restriction and sequence analysis of

the plasmid pVCAS confirmed its orientation and sequence.

Expression of His_6-tagged CyoA was performed using host *E. coli* BL21 (DE3) transformed with the plasmid pVCAS. An isolated colony was used to grow an overnight culture at 310 K in 50 ml of LB medium containing 100 µg ml^{-1} ampicillin. This culture was used to inoculate 1.5 l of induction medium and was grown at 310 K and 200 rev min^{-1}. When the culture reached log phase (OD_{600} = 0.5–0.7), expression was induced with 1 m*M* isopropyl β-D-thiogalactoside and the culture was incubated for 1 h before harvesting by centrifugation at 6 000*g*. The cells were resuspended in 3 ml of lysis buffer (50 m*M* NaH_2PO_4, 300 m*M* NaCl, 10 m*M* imidazole pH 8.0). Lysozyme (100 µl of 10 mg ml^{-1} solution per gram of cells) was added to the resuspended cells and incubated at 277 K for 1 h. To complete cell lysis, deoxycholic acid (4 mg per gram of cells) was added and incubated at 310 K for an additional 1 h. The sticky cell lysate was incubated with DNaseI (20 µl of 1 mg ml^{-1} solution per gram of cells) at room temperature until it was no longer viscous. A clear lysate was obtained by centrifugation (150 000*g*) and loaded onto an Ni–NTA column (Qiagen) which was equilibrated with lysis buffer (described above). Loosely bound proteins were eluted by washing with a minimum of eight bed volumes of wash buffer (50 m*M* NaH_2PO_4, 300 m*M* NaCl, 20 m*M* imidazole pH 8.0). Proteins were eluted with a 20–250 m*M* imidazole step gradient with a 10 m*M* increase per step. Histidine-tagged CyoA protein eluted between 100 and 130 m*M* imidazole. Fractions containing CyoA soluble domain were pooled and dialyzed against 50 volumes of 50 m*M* Tris–HCl pH 8.0. Proteins were concentrated to 10 mg ml^{-1} in a dialysis bag with solid PEG 8000 and stored at 193 K until required. At each step of the purification procedure, the protein size and purity was assessed using SDS–PAGE.

2.2. Crystallization

Hanging-drop vapor-diffusion methods were used for crystallization of CyoA soluble domain. An initial crystallization screen was performed using Hampton Research Crystal Screens 1 and 2 (Hampton Research) at room temperature. After refinement, 0.2 × 0.15 × 0.15 mm cubic shaped crystals formed after 2 weeks. The protein solution contained 8 mg ml^{-1} in 50 m*M* Tris base pH 8.0 and the reservoir solution consisted of 2 *M* ammonium sulfate and 5% 2-propanol. 10 µl of protein solution was mixed with 10 µl of reservoir solution and equilibrated against 1 ml of reservoir.

Table 1
Summary of crystallographic data.

Wavelength (Å)	1.0
Crystal system	Cubic
Space group	$P4_332$
Resolution (Å)	3.3
Total No. of observations	52232
Total No. of unique reflections	5077
Coverage completeness (%)	99.8
Outer range completeness (%)	100
R_{merge}†‡ (%)	4.3, 12, 43.2
$I/\sigma(I)$†	66, 31, 6

† The three values are for the inner (99–6.0 Å), complete (99–3.3 Å) and outer (3.51–3.3 Å) resolution ranges, respectively. ‡ $R_{merge} = \sum_{hkl}\sum_i |I_i - \langle I\rangle|/\sum_{hkl}\sum_i$, where $\langle I\rangle$ is the mean intensity of reflection *hkl*.

2.3. X-ray diffraction analysis

A crystal was transferred to cryoprotectant containing 20% PEG 2000, harvested in a nylon loop and cooled to cryogenic temperature (80 K) for data collection. Data were collected at 100 K at beamline 17-ID (IMCA-CAT) at the Advanced Photon Source (APS, Argonne, IL, USA). The crystal-to-detector distance was set to 200 mm and diffraction images were recorded with 1° oscillations per image and an exposure time of 20 s per frame on a 165 mm MARCCD detector. All data were processed and scaled using *XGEN* (Howard, 2000) (Table 1). The structure was determined by molecular replacement using *CNS* (Brünger *et al.*, 1998) and refined and rebuilt with *CNS* and *O* (Jones *et al.*, 1991).

3. Results and discussion

3.1. Cloning, expression and purification of *Vitreoscilla* CyoA soluble domain

The fragment encoding C-terminal CyoA soluble domain (residues 118–325) was cloned into pQE81 (Qiagen) for expression and single-step purification. When the expression level was tested, a significant degradation of the expressed protein was detected 1 h after induction; expression at various temperatures and IPTG concentrations produced similar results (data not shown). It is possible that highly expressed CyoA soluble protein could not be exported to the periplasmic space without its native signal sequence and was not stable in the *E. coli* cytosol. For this reason, the protein was induced only for 1 h, with the result that the enzyme was produced in good yield, giving 10 mg of pure protein per 1.5 l of cell culture with 1 h induction. Single-step purification was performed using Ni–NTA chromatography. Imidazole-gradient elution was applied to remove contamination and SDS–PAGE showed a single band at 24 kDa. The fusion protein containing a six-histidine tag at the N-terminal end of CyoA was directly used for crystallization without cleaving the tag.

3.2. Crystallization and crystallographic analysis

Initial crystallization conditions for the *Vitreoscilla* CyoA soluble domain using Hampton Research Crystal Screens 1 and 2 produced microcrystals (~30 µm) from only one well solution (2 *M* ammonium sulfate, 5% 2-propanol) with a protein concentration of 12 mg ml^{-1}. After several rounds of optimization attempts, 0.2 × 0.15 × 0.15 mm cubic crystals (Fig. 1*a*) were formed by reducing the protein concentration to 8 mg ml^{-1}. We co-crystallized the protein with the electron donor ubiquinol-1 and soaked pre-grown crystals in 3–10 m*M* solutions of ubiquinol 1; these experiments had no effect on the shape or diffraction quality of the crystals.

The crystals diffracted well at beamline 17-ID at the Advanced Photon Source; the

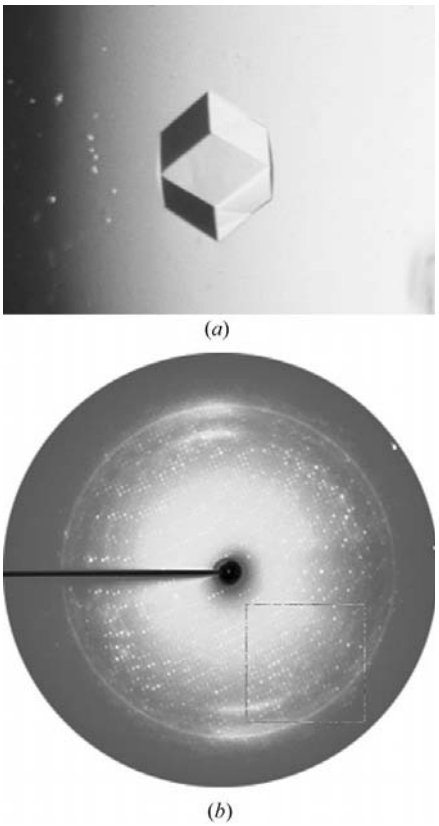

Figure 1
(*a*) A cubic crystal of *Vitreoscilla* CyoA soluble domain. (*b*) Diffraction pattern from a cubic crystal of *Vitreoscilla* CyoA soluble domain.

best crystal diffracted beyond 2.8 Å resolution (Fig. 1*b*). A single crystal was used to collect a native data set to 3.3 Å. Table 1 provides the data-collection statistics. The crystals belong to space group $P4_132$ or $P4_332$, with unit-cell parameters $a = b = c = 122.20$ Å, $\alpha = \beta = \gamma = 90^\circ$, giving a V_M value of 3.04 or a 60% solvent content, consistent with the presence of a single molecule (25 kDa including the six-residue histidine tag) in the asymmetric unit (Matthews, 1968).

3.3. Molecular replacement

Using all 15.0–4.0 Å data, cross-rotation functions were calculated by using the fast direct rotation search of *CNS*. The search model was prepared from the structure of the periplasmic fragment of quinol oxidase from *E. coli* (PDB code 1cyw; Wilmanns *et al.*, 1995). The pairwise comparison between the 159 amino acids (residues 125–283) in 1cyw and the corresponding *Vitreoscilla* CyoA soluble domain used in this study indicates 43 identical residues (27% identity). The soluble domain contains six extra residues at the N-terminus, excluding the histidine tag: 16 residues between residues 257 and 258 in 1cyw and 29 residues at the C-terminus. All non-glycine residues in the search model were changed to alanine residues and all *B* values were set to the search model's average value of 28.9 Å^2. With the relatively low-resolution data (3.3 Å) of the *Vitreoscilla* data, Wilson statistics may not be able to estimate an adequate overall *B* factor. The top ten peaks from the fast direct rotation search (mean, 0.0259; std, 0.0068; top ten peak range, 0.0390–0.0334) were used for the translation search, since often the top peak does not represent the best solution and more than one peak can give rise to a solution. The best solution, which arose from the highest cross-rotation function peak, appeared at (θ_1, θ_2, θ_3, x, y, z) = (67.24, 9.73, 73.85, 45.02, 15.90, −15.20). At this position, the correlation function value ('monitor') was 0.371 and the fraction of the asymmetric unit occupied by the model ('packing') was 0.3851. The mean of the monitor values for the top ten solutions was 0.3438 ± 0.02051. The monitor values for the next few inferior translation solutions were 0.369–0.362; these values differ from the best solution by less than 0.5σ, necessitating visual inspection of these solutions. Our visual analysis of these translation solutions using the program *O* indicated that only the best solution showed no apparent collision between symmetry-related molecules. The initial model gave an *R* value of 0.43 and an R_{free} of 0.45. A few rounds of grouped *B*-value refinements and minimizations in *CNS* against 3.3 Å data and manual adjustment using *O* reduced the *R* value and R_{free} to 0.32 and 0.40, respectively. In the grouped *B*-value refinement, atoms are grouped in either main-chain atoms (C, N, O, C^α) or side-chain atoms. Each minimization step included 200 minimization cycles with a maximum-likelihood target using amplitudes. Side-chain atoms were added when electron density appeared as the refinement progressed. The latest refinement suggested additional electron density for several residues which were not included in the search model. This suggests that the solution is correct. While the refinement is progressing well with our current data to 3.3 Å, we are working to obtain better diffracting crystals in the hope of obtaining a higher resolution structure.

Data were collected at beamline 17-ID in the facilities of the Industrial Macromolecular Crystallography Association Collaborative Access Team (IMCA-CAT) at the Advanced Photon Source. These facilities are supported by the companies of the Industrial Macromolecular Crystallography Association through a contract with Illinois Institute of Technology (IIT), executed through IIT's Center for Synchrotron Radiation Research and Instrumentation. Use of the Advanced Photon Source was supported by the US Department of Energy, Basic Energy Sciences, Office of Science under Contract No. W-31-109-Eng-38.

References

Brünger, A. T., Adams, P. D., Clore, G. M., DeLano, W. L., Gros, P., Grosse-Kunstleve, R. W., Jiang, J. S., Kuszewski, J., Nilges, M., Pannu, N. S., Read, R. J., Rice, L. M., Simonson, T. & Warren, G. L. (1998). *Acta Cryst.* D**54**, 905–921.

Calhoun, M. W., Thomas, J. W. & Gennis, R. B. (1994). *Trends Biochem. Sci.* **19**, 325–330.

Efiok, B. J. S. & Webster, D. A. (1990*a*). *Biochemistry*, **29**, 4734–4739.

Efiok, B. J. S. & Webster, D. A. (1990*b*). *Biochem. Biophysics. Res. Commun.* **173**, 370–375.

Gennis, R. B. (1991). *Biochim. Biophys. Acta*, **1058**, 21–24.

Georgiou, C. D., Cokic, P., Carter, K., Webster, D. A. & Gennis, R. B. (1988). *Biochem. Biophys. Acta*, **933**, 179–183.

Georgiou, C. D. & Webster, D. A. (1987). *Biochemistry*, **26**, 6521–6526.

Gohlke, U., Warne, A. & Saraste, M. (1997). *EMBO J.* **16**, 1181–1188.

Howard, A. J. (2000). In *Crystallographic Computing 7: Proceedings of the Macromolecular Crystallographic Computing School*, edited by P. E. Bourne & K. D. Watenpaugh. Oxford University Press.

Jones, T. A., Zou, J. Y., Cowan, S. W. & Kjeldgaard, M. (1991). *Acta Cryst.* A**47**, 110–119.

Kim, K. J., Chi, P. Y., Hwang, K. W., Stark, B. C. & Webster, D. A. (2000). *J. Biochem.* **128**, 49–55.

Kita, K., Konishi, K. & Anraku, Y. (1984). *J. Biol. Chem.* **259**, 3368–3374.

Ma, J., Puustinen, A., Wikström, M. & Gennis, R. B. (1998). *Biochemistry*, **37**, 11806–11811.

Matsushita, K., Patel, L. & Kaback, H. R. (1984). *Biochemistry*, **23**, 4703–4714.

Matthews, B. W. (1968). *J. Mol. Biol.* **33**, 491–497.

Saraste, M., Raitio, M., Jalli, T., Chepuri, V., Lemieux, L. & Gennis, R. B. (1988). *Ann. NY Acad. Sci.* **550**, 314–324.

Sato-Watanabe, M., Mogi, T., Sakamoto, K., Miyoshi, H. & Anraku, Y. (1998). *Biochemistry*, **37**, 12744–12752.

Trumpower, B. L. & Gennis, R. B. (1994). *Annu. Rev. Biochem.* **63**, 675–716.

Tsatsos, P. H., Reynolds, K., Nickels, E. F., He, D.-Y., Yu, C.-A. & Gennis, R. B. (1998). *Biochemistry*, **37**, 9884–9888.

Wilmanns, M., Lappalainen, P., Kelly, M., Sauer-Eriksson, E. & Saraste, M. (1995). *Proc. Natl Acad. Sci. USA*, **92**, 11955–11959.